Beat over the Old Ground with New Strategy: Engineering As···As Interaction in Arsenite-Based Dawson Cluster β-[W$_{18}$O$_{54}$(AsO$_3$)$_2$]$^{6-}$

Qiuxia Han,*,[†] Xueping Sun,[‡] Jie Li,[†] Pengtao Ma,[†] and Jingyang Niu*,[†]

[†]Institute of Molecular and Crystal Engineering, School of Chemistry and Chemical Engineering, Henan University, Kaifeng 475004, People's Republic of China

[‡]Department of Environmental Engineering and Chemisty, Luoyang Institute of Science and Technology, Luoyang 471023, People's Republic of China

S Supporting Information

ABSTRACT: By reaction of [As$_2$W$_{19}$O$_{67}$(H$_2$O)]$^{14-}$, NiCl$_2$·6H$_2$O, and phen under hydrothermal conditions, a new organic–inorganic tungstoarsenate hybrid [Ni(phen)$_3$]$_4$[As$_2$W$_{18}$O$_{60}$]{[Ni(phen)$_2$][H$_2$As$_2$W$_{18}$O$_{60}$]}·12H$_2$O (where phen = 1,10-phenanthroline) (**1**) was obtained via self-assembly and characterized by elemental analysis, infrared (IR) spectroscopy, solid UV−vis absorption spectrum, and single-crystal X-ray diffraction (XRD). An unprecedented 18-tungstoarsenate Dawson cluster, β-[W$_{18}$O$_{54}$(AsO$_3$)$_2$]$^{6-}$, encapsulating two pyramidal arsenite AsO$_3^{3-}$ anions as templates and exhibiting interesting intramolecular As···As interaction is first achieved. **1** displays a one-dimensional (1D) chain architecture constructed by alternating β-[W$_{18}$O$_{54}$(AsO$_3$)$_2$]$^{6-}$ and nickel(II) complexes [Ni(phen)$_2$]$^{2+}$. The resulting hybrid can act as a photocatalyst to prompt the degradation of Rhodamine B (RhB) with excellent efficiency.

Impossible? NO!

[As$_2$W$_{19}$O$_{67}$(H$_2$O)]$^{14-}$ → β-[W$_{18}$O$_{54}$(AsO$_3$)$_2$]$^{6-}$
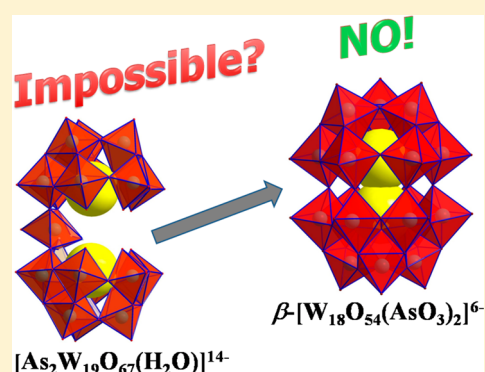
INTRODUCTION

Polyoxometalates (POMs) are a large family of well-known polynuclear metal-oxo clusters consisting of Group V and VI metals (M = W, Mo, V, Nb, etc.) in their highest oxidation states with an unmatched structure variety, which can be finely tuned by choice of constituent elements and countercations.[1,2] In recent years, POMs have attracted great attention to material chemistry and displayed potential applications in catalysis, because of their thermal and oxidative stability, redox potentials, (multi)electron-transfer properties, acidities, and solubilities.[3−5] Besides the best known Keggin POMs, Well–Dawson structures representing the very notable and stable subset of POM-based clusters have received extensive development since their initial discovery 60 years ago.[6−8] Well–Dawson structures can be classified into two types: the conventional Dawson-type POMs [M$_{18}$O$_{54}$(XO$_4$)$_2$]$^{n-}$ (where M = Mo, W, and X is a main-group element) incorporate two tetrahedral anions such as PO$_4^{3-}$,[9] AsO$_4^{3-}$,[10] SO$_4^{2-}$,[11] or ClO$_4^{-}$.[12] Compared to the abundant reported conventional Dawson-type POMs, only a few examples of unconventional Dawson clusters hosting nontetrahedral anions, such as a ditetrahedral anion P$_2$O$_7^{4-}$ (two tetrahedral sharing one corner, as in (Bu$_4$N)$_4$[Mo$_{18}$O$_{54}$(P$_2$O$_7$)]),[13] a trigonal-prismatic anion IO$_6^{6-}$ or TeO$_6^{6-}$ (as in [H$_3$W$_{18}$O$_{56}$(XO$_6$)]$^{6-}$),[14,15] or a pyramidal BiO$_3^{3-}$ or AsO$_3^{3-}$ (a single unit in the cluster and two protons occupy the heteroatomic vacant site, as in [W$_{18}$O$_{54}$(AsO$_3$)(H)$_2$O$_3$]$^{7-}$).[16,17]

A survey of the available literatures shows that it is difficult to incorporate two pyramidal XO$_3^{3-}$ in each cluster simulta-

neously, presumably because two lone pairs of two heteroatoms would point toward each other, thus preventing such an association (X$_2$W$_{18}$).[15−17] However, Cronin and co-workers reported a new family of Dawson-type 18-molybdosulfites and tungstosulfites that encapsulate two pyramidal sulfite SO$_3^{2-}$ anions as the central cluster templates which exhibit interesting intramolecular S···S interactions.[18] Inspired by the above excellent work, we expect to introduce a new unconventional Dawson cluster incorporating two pyramidal AsO$_3^{3-}$, because arsenite is analogous to sulfite and inclined to form chemical bonds between atoms. This type of phenomenon commonly exists in inorganic compounds, such as skutterudite As$_4^{3-}$ (with an As···As bond of 3.14 Å) and realgar As$_4$S$_4$ (with an As–As bond of 2.45 Å).[19,20] We envisioned that the unconventional Dawson cluster incorporating two pyramidal AsO$_3^{3-}$ in each cluster simultaneously may exhibit unprecedented properties arising from the interesting intramolecular interacation between the encapsulated sulfite anions, thus providing a new way to regulate the physical properties of Dawson clusters.
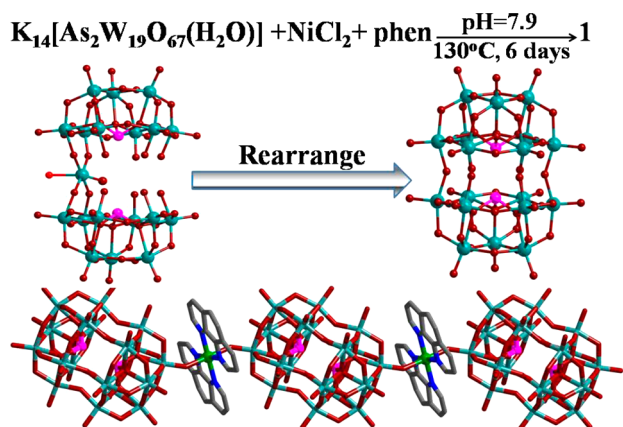
The dilacunary tungstoarsenate(III) [As$_2$W$_{19}$O$_{67}$(H$_2$O)]$^{14-}$ (abbreviated as {As$_2$W$_{19}$}), which is constructed of B-α-[AsW$_9$O$_{33}$]$^{9-}$ units linked together by additional tungsten, is a potential suitable precursor and may rearrange during the course of the reaction to get "unexpected" or "unusual" structural features.[21,22] We envisioned that the {As$_2$W$_{19}$} units may hold back the [AsW$_9$O$_{33}$]$^{9-}$ in the rearrangement of the

reaction to form an unconventional 18-tungstoarsenate Dawson cluster. In addition, organic groups that have been introduced can act as structure-stabilizing agents to enhance the stability of formed organic−inorganic hybrid fragments. More importantly, the hydrothermal environment is able to make the reaction shift from the thermodynamic to the kinetic, so that tungstoarsenate precursor can be rearranged, which provides a necessary precondition for constructing new fragments. By selecting $\{As_2W_{19}\}$ as starting material to react with TM cation in the organic components under hydrothermal conditions, herein, we report the design and synthesis of a new organic−inorganic POM hybrid: $[Ni(phen)_3]_4[As_2W_{18}O_{60}]\{[Ni(phen)_2]-[H_2As_2W_{18}O_{60}]\}\cdot12H_2O$, abbreviated as $\{[Ni(phen)_2]-[H_2As_2W_{18}O_{60}]\}$ (**1**). Fortunately, an unconventional 18-tungstoarsenate Dawson cluster β-$[W_{18}O_{54}(AsO_3)_2]^{6-}$ (**1a**) that encapsulates two pyramidal arsenite AsO_3^{3-} anions as templates was first obtained (Scheme 1). Similar to the sulfite-

Scheme 1. Synthetic Procedure of 1, Showing the Rearrangement of Precursor $\{As_2W_{19}\}$ and the 1D Chain Architecture Constructed by Alternating β-$[W_{18}O_{54}(AsO_3)_2]^{6-}$ Anions and Nickel(II) Complexes $[Ni(phen)_2)]^{2+a}$

$$K_{14}[As_2W_{19}O_{67}(H_2O)] + NiCl_2 + phen \xrightarrow[130^\circ C,\ 6\ days]{pH=7.9} 1$$

Rearrange

[a]Color legend: green, Ni^{2+}; gray, C; blue, N; dark red, O; and teal, W. For the sake of clarity, the H atoms have been omitted.

based Dawson cluster β-$[Mo_{18}O_{54}(SO_3)_2]^{4-}$,[18a] a short intra-molecular As···As interaction between the two anions in the β-$[W_{18}O_{54}(AsO_3)_2]^{6-}$ skeleton is also observed.

■ EXPERIMENTAL SECTION

General Methods and Materials. All reagents were of reagent-grade quality, obtained from commercial sources, and used without further purification. $K_{14}[As_2W_{19}O_{67}(H_2O)]\cdot30H_2O$ was prepared according to the literature method.[21] Elemental analyses (EA) of C, H, and N were performed on a Vario ELIII elemental analyzer. Inductively coupled plasma (ICP) analysis was performed on a Jarrel−Ash Model J-A1100 spectrometer. Powder XRD was obtained on a Rigaku Model D/Max-2400 X-ray diffractometer with a sealed copper tube (λ = 1.54178 Å). The infrared (IR) spectrum was recorded from a sample powder pelletized with KBr on a Nicolet Model 170 SXFT-IR spectrometer over a range of 4000−400 cm^{-1}. Solid UV−vis absorption spectrum was collected on a Hitachi Model U-4100 UV−vis spectrometer from 200 to 900 nm with a 60-mm-diameter integrating sphere at room temperature.

Synthesis of $[Ni(phen)_3]_4[As_2W_{18}O_{60}]\{[Ni(phen)_2[H_2As_2W_{18}O_{60}]\}\cdot12H_2O$ (1). A mixture of $K_{14}[As_2W_{19}O_{67}(H_2O)]\cdot30H_2O$ (0.5821 g, 0.1 mmol), $NiCl_2\cdot6H_2O$ (0.1188 g, 0.5 mmol), and phen (0.1264 g, 0.7 mmol) in 10 mL of distilled water was stirred and its pH value was

adjusted to 7.9 with 1 mol L^{-1} NaOH. The resulting suspension was sealed in a 25-mL Teflon-lined reactor and maintained at 130 °C for six days. After cooling the autoclave to room temperature, light green rodlike single crystals were separated, washed with water, and air-dried (60% yield, based on $\{As_2W_{19}\}$). EA and ICP (%) calcd for $C_{168}H_{134}As_4N_{28}Ni_5O_{130}W_{36}$: C 17.05, H 1.14, N 3.31, Ni 2.48, As 2.53, W 55.91; Found: C 17.14, H 1.08, N 3.24, Ni 2.58, As 2.47, W 55.83. IR (KBr): ν = 3440 (br, s), 1622 (s), 1518 (s), 1430 (s), 1145 (w), 1106 (w), 955 (s), 890 (s), 850 (w), 797 (vs) cm^{-1}.

X-ray Crystallographic Analysis. Intensity data for **1** were collected on a Bruker SMART APEX CCD diffractometer with graphite-monochromated Mo Kα (λ = 0.71073 Å), using the SMART and SAINT programs.[23,24] Routine Lorentz polarization and Multiscan absorption correction were applied to the intensity data. The structure was determined and the heavy atoms were found via direct methods, using the SHELXTL-97 program package.[25] The remaining atoms were found from successive full-matrix least-squares refinements on F^2 and Fourier syntheses. Except for a few oxygen and carbon atoms, other non-hydrogen atoms were refined anisotropically. Hydrogen atoms within the ligand backbones were fixed geometrically at their positions and allowed to ride on the parent atoms. Crystallographic data for **1** are summarized in Table 1. Selected atomic coordinates and

Table 1. Crystallographic Data and Structural Refinement for 1

parameter	value
empirical formula	$C_{168}H_{134}As_4N_{28}Ni_5O_{130}W_{36}$ (**1**)
mol wt, M [g mol^{-1}]	11836.86
crystal system	monoclinic
space group	$P2(1)/c$
a [Å]	17.186(2)
b [Å]	33.138(4)
c [Å]	23.420(3)
β [deg]	106.093(2)
V [Å^3]	12815(3)
Z	2
D_{calcd} [g cm^{-3}]	3.068
T [K]	296(2)
refl. collected/unique	65322/22427 [$R_{(int)}$ = 0.0732]
refl. observed	14100
m [mm^{-1}]	17.045
$F(000)$	10628
limiting indices	$-20 \leq h \leq 20$, $-39 \leq k \leq 32$, $-26 \leq l \leq 27$
$R_1{}^a$ [$I > 2\sigma(I)$]	0.0711
$wR_2{}^b$ [$I > 2\sigma(I)$]	0.1835
$R_1{}^a$ (all data)	0.1243
$wR_2{}^b$ (all data)	0.2053
diff peak and hole, eÅ^{-3}	4.506/−3.573

[a]$R_1 = \sum\|F_0| - |F_c\|/\sum|F_0|$. [b]$wR_2 = [\sum w(F_0{}^2 - F_c{}^2)^2/\sum w(F_0{}^2)^2]^{1/2}$; $w = 1/[\sigma^2(F_0{}^2) + (xP)^2 + yP]$, $P = (F_0{}^2 + 2F_c{}^2)/3$, where x = 0.1109 and y = 194.8345 for **1**.

equivalent isotropic displacement parameters are listed in Table S1 in the Supporting Information. Selected bond lengths and angles of **1** are listed in Table S2 in the Supporting Information.

Catalysis. The photocatalytic activity of the catalyst **1** was tested using RhB as the target through the following approach.[26] A 5-mL RhB solution (2×10^{-5} mol L^{-1}, 9.6 mg L^{-1}) was added into a quartz test tube. Then, 10 mg of catalyst **1** was suspended into the RhB solution and the suspension was ultrasonically dispersed for 5 min. The RhB solution was then irradiated under a CHF-XM35−500W xenon lamp (Beijing Trusttech Co. Ltd., Beijing, PRC) with intense stirring. The temperature was maintained at 20 °C by the circulation of cool water. The degradation of RhB was followed by monitoring of the decrease in absorbance at 544 nm, which is due to the cleavage of the aromatic ring of the RhB dye. The reaction mixture was withdrawn at
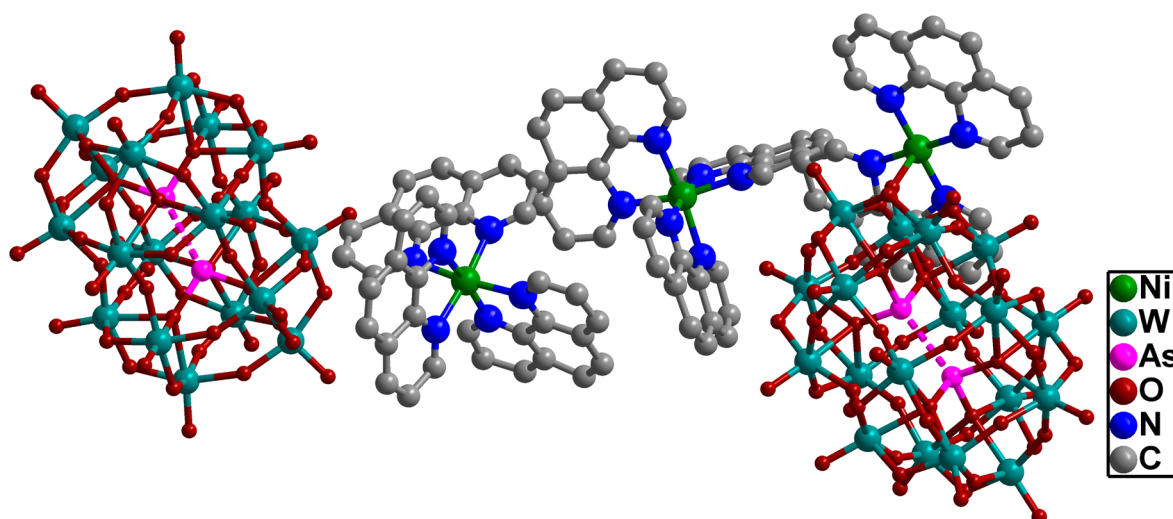
Figure 1. Ball-and-stick representation of **1** in an asymmetric unit. H atoms and H_2O molecules are omitted for the sake of clarity.

regular intervals to study the progress of the reaction. In a typical operation, 30 μL of solution was taken out with the help of a microsyringe and then was injected into 3 mL of a water solution. The concentration of RhB is calculated by a calibration curve. The degradation efficiency can be calculated as

$$\text{efficiency}\,(\%) = \frac{C_0 - C_t}{C_0} \times 100$$

where C_0 is the initial concentration of RhB and C_t is the revised concentration after given time intervals.

■ RESULTS AND DISCUSSION

Synthesis. **1** was hydrothermally synthesized by a mixture of $\{As_2W_{19}\}$, $NiCl_2 \cdot 6H_2O$, and phen in distilled water. Elemental analysis (EA) and powder XRD indicated the pure phase of its bulk sample. (See Figure S2 in the Supporting Information.) The pH value has great influence on the isolation of product phases in our case. Parallel experiments revealed that the pH value of the system varied over a range of 7.0–7.9, which favored the formation of **1**. In addition, the organic ligand and transition-metal cation play great roles in the formation of product phases. When phen was replaced by dap (dap = 1,2-diaminopropane), tetra-Ni sandwich-typed [Ni-$(dap)_2H_2O]_2\{[Ni(dap)]_2[Ni_2(dap)_2Ni_2(HAs^VW_9O_{34})_2]\}$ · $9H_2O$ was obtained at pH 6.5.[27] When the Ni^{2+} cation was replaced by the Cu^{2+} cation in the participation of phen at pH 5.5, hexa-Cu sandwich-typed $[Cu_2(phen)_2(\mu\text{-ox})]\{[Cu(phen)\text{-}$ $(H_2O)_2][Cu_4(H_2O)_4Cu_2(phen)_2(As^{III}W_9O_{33})_2]\} \cdot 6H_2O$ was obtained.[28] When the Ni^{2+} cation was replaced by the Fe^{3+} cation in the participation of ethylenediamine (en), another new S-shaped structure $(enH_2)_2[Fe_2]\{(HAs^VW_6O_{26})\text{-}$ $[Fe_3(H_2O)](H_5As^VW_9O_{34})\}_2 \cdot 8H_2O$ was synthesized.[29] These results indicate the $\{As_2W_{19}\}$ precursor tends to transform to $[B\text{-}\alpha\text{-}AsW_9O_{34}]^{9-}$, $[\alpha\text{-}AsW_6O_{26}]^{11-}$, or $[B\text{-}\alpha\text{-}AsW_9O_{33}]^{9-}$ fragments under hydrothermal conditions and is favored to rearrange to new POM fragments for constructing much more-novel POMs. Therefore, systematic exploration on this system still remains a great challenge to us, and this work is in progress.

Structural Description. Single-crystal structural analysis revealed that **1** crystallized in a space group $P2(1)/c$. The molecular asymmetric unit of **1** consists of two crystallographically independent 18-tungstoarsenate Dawson β-

$[W_{18}O_{54}(AsO_3)_2]^{6-}$, five hexa-coordinated nickel cations ($[Ni\text{-}$ $(phen)_3]^{2+}$ and $[Ni(phen)_2(O_t)_2]^{2+}$), 12 water molecules of crystallization, and two protons, based on charge balance (see Figure 1). One of the two independent Dawson 18-tungstoarsenates $\beta\text{-}[W_{18}O_{54}(AsO_3)_2]^{6-}$ connects one $[Ni\text{-}$ $(phen)_2]^{2+}$ by two terminal oxygen of polyanions alternatively to produce a one-dimensional (1D) chainlike structure. The others nickel(II) ions were coordinated in octahedral geometries with six nitrogen atoms from three phen ligands.

Interestingly, the $\beta\text{-}[W_{18}O_{54}(AsO_3)_2]^{6-}$ anion has an overall approximate D_{3d} symmetry, with a staggered arrangement of the AsO_3 moieties, in contrast to the eclipsed arrangements in $\alpha\text{-}[Mo^{VI}_{18}O_{54}(SO_3)_2]^{4-}$ with a mirror plan dividing the cage into two equal parts linked together by six equatorial oxo ligands and with D_{3h} symmetry (see Figure 2).[18a] The distinctive peanutlike shape of the $\{W_{18}O_{54}\}$ framework was also observed for $\{Mo_{18}O_{54}\}$ cages in the Dawson-type compound $(C_{16}H_{36}N)_4[Mo_{18}O_{54}(SO_3)_2] \cdot C_2H_3N$[18a] and the other tungstate compounds $(Bu_4N)_6[W_{18}O_{54}(OH)_3(BiO_3)]$[16] and $(H_4N)_7[W_{18}O_{54}(O)(OH)_2(AsO_3)]$.[17] There are significant differences from traditional classical datepit-like Dawson polyanion $\alpha\text{-}[As_2W_{18}O_{62}]^{6-}$ (see Figure 2b):[10]

(1) The classical Wells–Dawson structure can be rationalized as two A-type trilacunary Keggin subunits fused, whereas the unconventional can be seen as being composed of two B-type trilacunary Keggin subunits;

(2) The classical Wells–Dawson structure possesses 62 oxygen atoms, rather than 60;

(3) The classical Wells–Dawson structure holds two tetrahedral anions, rather than two pyramidal anions;

(4) The classical Wells–Dawson structure has two μ_4-oxo and six μ_3-oxo atoms, rather than six μ_4-oxo atoms; and

(5) Particularly, the capping fragments in the classical structure are W_3O_{13} trimers of edge-sharing WO_6 octahedra, whereas the capping fragments in the unconventional structure are W_3O_{15} triads of corner-sharing octahedra.

In the skeleton of the $\beta\text{-}[W_{18}O_{54}(AsO_3)_2]^{6-}$ moiety, two pyramidal arsenite AsO_3^{3-} anions still reside in the central of the moiety and share three oxygen atoms with three $\{W_3O_{13}\}$ triad with As–O distances from 1.76(1) Å to 1.80(2) Å and O–As–O angles from 99.4(6)° to 100.7(7)° (see Table 2). As
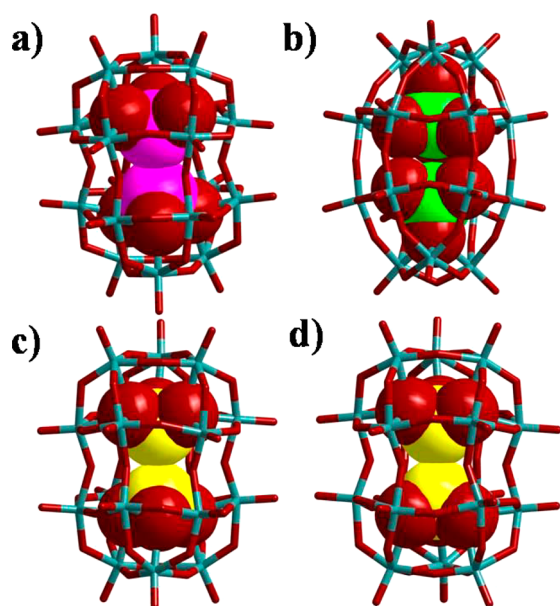
Figure 2. Schematic representation of the structures of the Dawson clusters: (a) arsenite-based Dawson cluster in **1**: β-$[W_{18}O_{54}(AsO_3)_2]^{6-}$; (b) a comparison with the conventional arsenate-based Dawson anion α-$[W_{18}O_{54}(AsO_4)_2]^{6-}$;[10] (c) sulfite-based Dawson cluster: β-$[Mo_{18}O_{54}(SO_3)_2]^{4-}$;[18] (d) sulfite-based Dawson cluster: α-$[Mo_{18}O_{54}(SO_3)_2]^{4-}$,[18] whereby the central anion templates are shown in a space-filling mode. (Color legend: violet, As^{3+}; yellow, S^{4+}; green, As^{5+}; dark red, O; and teal, W and Mo.)

expected, the average As−O distance (1.78 Å) and the corresponding average O−As−O angles (100.1°) in **1a** are 0.09 Å shorter (1.87 Å) and 2.6° larger (97.5°) than that in $(H_4N)_7[W_{18}O_{54}(O)(OH)_2(AsO_3)]$, respectively.[17] The significant difference may be beneficial for simultaneously holding two AsO_3 anions in the cage. Meanwhile, the fact that the equivalent isotropic displacement parameters (U(eq), Å^2) for both As(1) and As(2) of the clusters are ∼0.020(1) and 0.031(1) give preliminary crystallographic evidence to support this structure (see Table S1 in the Supporting Information). A novel aspect of this work, similar to the sulfite Dawson cluster anions reported,[18] is the short As···As contact resulting from the incorporation and relative orientation of the two arsenite ions within the {W18} cage. The As···As distance of 3.09(3) Å is much shorter than the sum of the van der Waals radii of two arsenic atoms (ca. 3.70 Å).

Dawson anions are well-known to possess interesting electrochemical and multielectron transfer properties.[30] We envisioned that the unconventional Dawson cluster β-$[W_{18}O_{54}(AsO_3)_2]^{6-}$ incorporating two pyramidal AsO_3^{3-} in a configuration causing a short, yet nonbonding intramolecular As···As interaction between the {AsO3} anions may exhibit unprecedented properties arising from the interesting intramolecular interaction between the encapsulated sulfite anions. Cronin and co-workers reported Dawson-type 18-molybdosulfites that encapsulated two pyramidal sulfite SO_3^{2-} exhibited unusual reversible thermochromic properties over the temperature range of 77−500 K.[18a] Thus, we expected that the incorporation of nontetrahedral arseniteions in **1** could further extend their versatility. A search of the structure revealed that there are many structures reported for dithionates $S_2O_6^{2-}$ and diphosphates $P_2O_6^{4-}$ ions.[31,32] However, none of the $As_2O_6^{4-}$ analogues have been reported, which should be existence according to the property similarity of chemical elements from the same clan in the periodic table.[19] Therefore, we speculate that the arsenite anions may undergo redox processes, similar to the sulfite anions, at least theoretically involving their oxidation to diarsenate $As_2O_6^{4-}$ ions (reaction 1),

$$2AsO_3^{3-} \rightarrow As_2O_6^{4-} + 2e^- \tag{1}$$

This process could supply two electrons to reduce the surrounding polyoxotungstate shell to the mixed-valence reduction state $\{W^{VI}_{16}W^{V}_{2}\}$ with its characteristic blue color, if it was possible to form a diarsenate anion. Yet, the formation of a As···As single bond within the systems presented here appears to be restricted by the large geometrical changes required of the {W18} framework, since the As···As distance would have to decrease from ∼3.09 Å to ∼2.20 Å. The thermochromic property of **1** was also investigated over the temperature range of 77−500 K; however, only a slight color change occurs, from light green (300 k) to green (500 k), which maybe due to the reducibility of tungsten(VI), which is much weaker than that of molybdenum(VI). There is a certain new property arising from the intramolecular electronic interaction between the encapsulated anions, but the test data show few useful results and this work has yet to be further researched.

IR and UV Spectra. The IR spectrum of **1** displays the characteristic vibration patterns derived from the Keggin framework $[B-AsW_9O_{33}]^{9-}$ (see Figure S3 in the Supporting Information). Four characteristic vibration bands, namely,

Table 2. As−O Bond Lengths and As−O−As Angles of 1, Compared to Those of $[W_{18}O_{54}(AsO_3)(H)_2O_3]^{7-a}$

bond	length (Å)	angle	measurement (°)
As(1)−O(11)	1.76(1)	O(11)−As(1)−O(15)	99.4(6)
As(1)−O(15)	1.77(1)	O(11)−As(1)−O(6)	100.0(6)
As(1)−O(6)	1.80(2)	O(15)−As(1)−O(6)	100.5(6)
As(2)−O(35)	1.77(2)	O(35)−As(2)−O(44)	100.2(8)
As(2)−O(44)	1.78(2)	O(35)−As(2)−O(40)	100.7(7)
As(2)−O(40)	1.80(2)	O(44)−As(2)−O(40)	99.7(7)
As(1)···As(1A)^b	3.09(3)		
As(2)···As(2B)^b	3.07(3)		
Average length (Å)		**Average angle (°)**	
in **1**	1.78	in **1**	100.1
in $[W_{18}O_{54}(AsO_3)(H)_2O_3]^{7-}$	1.87	in $[W_{18}O_{54}(AsO_3)(H)_2O_3]^{7-}$	97.5

^{a}Data obtained from ref 17. ^{b}Symmetry code: A: $4 − x$, $2 − y$, $1 − z$; B: $1 − x$, $−y$, $2 − z$.
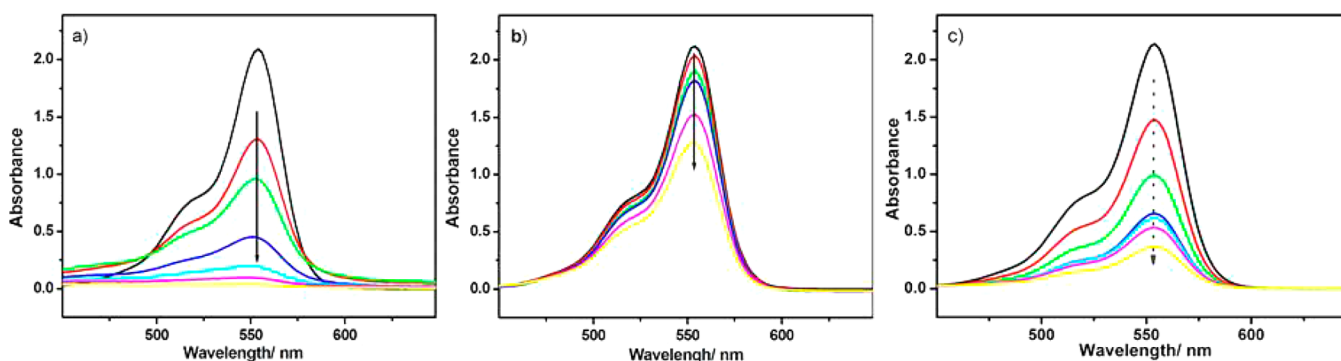
Figure 3. Temporal UV-vis absorption spectral changes observed for the RhB solutions, as a function of irradiation time: (a) in the presence of 10 mg of **1**; (b) the absence of any catalyst (the control experiment); and (c) in the presence of 4 mg of $K_6As_2W_{18}O_{62}\cdot9H_2O$.

ν(W−Ot), ν(W−Ob), ν(As−Oa) and ν(W−Oc), appear at 955, 890, 850, and 797 cm^{-1}, respectively. In comparison with those of {As$_2$W$_{19}$}, the W−Ot, As−Oa, and W−Oc vibration bands in **1** have different blue-shifts, which further confirmed the rearrangement of the structure. In addition, the vibration peaks from 1106 cm^{-1} to 1622 cm^{-1} are indicative of phen ligands.[8] The occurrence of these resonance signals confirms the presence of phen and water molecules, being in good agreement with the single-crystal structural analysis.

As can be seen from Figure S4 in the Supporting Information, the solid UV-vis absorption spectrum of **1** exhibits excellent light absorption properties in the 190−700 nm range (two strong absorption wavelength centered at 190 and 300 nm and a broad adsorption in the visible range (550 nm)) with BaSO$_4$ as a background. The two strong bands near 190 and 300 nm are attributed to the ligand-to-metal charge transfers of O$_t$→W and O$_{b,c}$→W, respectively, where electrons are promoted from the low-energy electronic states (mainly comprising O 2p orbits) to the high-energy states (mainly comprising metal d orbits).[8] The broad band near 550 nm corresponds to typical metal-to-ligand charge transfer (MLCT) from a low-oxidation-state Ni^{2+} ion to the low-energy π^* orbits of phen.

Catalysis. In recent years, POMs have been considered as efficient photocatalysts for removing organic dyes from wastewater,[33−35] because of the similar photocatalytic characteristics to semiconductors.[36] However, compared with TiO$_2$ and ZnO, POMs show high solubility in water and it is difficult to recover the photocatalyst from the solvent for reuse.[37] On the other hand, the photodegradation of dye pollutants by POMs is mainly driven by UV light; however, the UV light only accounts for ∼5% of sunlight, which limits the application of POMs as a photocatalyst. The design of a highly active and recyclable heterogeneous catalyst is expected for effective applications for the degradation of organic dyes.

Taking into consideration the broad adsorption of **1** in the UV-vis region, the photocatalytic property of **1** toward a Rhodamine B (RhB) solution was also investigated through a heterogeneous process. The absorption spectra of RhB aqueous solution at different irradiation times during the photodegradation process are shown in Figure 3; and the decrease of absorption intensity from 2.09 to 0.04 within 6 h at λ_{max} = 554 nm indicates the degradation of RhB molecules. During the sunlight irradiation process, no new absorption peaks appeared and the absorption maximum of the solution did not exhibit a significant hypsochromic shift in the 500−600 nm regions. This confirms the absence of N-de-ethylation of RhB. Therefore, the

decrease in the absorbance was due to the cleavage of the aromatic ring of the RhB dye. In addition, the color of the RhB in an aqueous solution changed from rose-bengal to almost colorless after sunlight irradiation for 6 h, which indicated almost-complete degradation of RhB. A control experiment without catalyst showed that the absorption peak of RhB obviously decreased from 2.20 to 1.28 under similar conditions. The conversion of the RhB calculation result showed that the conversion of RhB was significantly improved by **1**, from 41.8% to 98.1%. It should be noted that catalyst **1** is more superior to the previously known $K_6As_2W_{18}O_{62}$ homogeneous catalyst, which exhibits a 82.8% decolorization rate for RhB solution under the same conditions.[38] It may be deduced that **1** can be induced by visible light and improve the efficiency of visible light. In addition, crystals of **1** were easily isolated from the reaction suspension by filtration alone and reused three times, displaying only a slight decrease in activity (see Table S3 in the Supporting Information). These results suggest that **1** may be a potential heterogeneous photocatalyst with photocatalytic activities in the reduction of some other organic dyes.

CONCLUSIONS

In summary, a new organic−inorganic hybrid exhibiting a heterogeneous catalytic performance for degradation of Rhodamine B (RhB) under sunlight in an aqueous solution was achieved. It is worth mentioning that [Ni-(phen)$_3$]$_4$[As$_2$W$_{18}$O$_{60}$]{[Ni(phen)$_2$][H$_2$As$_2$W$_{18}$O$_{60}$]}·12H$_2$O (where phen = 1,10-phenanthroline) (**1**) displays a one-dimensional (1D) chain architecture constructed by alternating nickel(II) complexes [Ni(phen)$_2$)]$^{2+}$ and unprecedented 18-tungstoarsenate Dawson cluster, β-[W$_{18}$O$_{54}$(AsO$_3$)$_2$]$^{6-}$, which encapsulates two pyramidal arsenite AsO$_3^{3-}$ anions as templates and exhibits interesting intramolecular As···As interaction between the two anions. It endows us with great opportunities and considerable challenges in designing and creating novel hybrid POM materials.

ASSOCIATED CONTENT

ⓈSupporting Information

Crystal data in CIF format. Tabular data given in PDF format. This material is available free of charge via the Internet at http://pubs.acs.org.

AUTHOR INFORMATION

Corresponding Authors

*Tel./Fax: (+86)-378-3886876. E-mail:hdhqx@henu.edu.cn (Q.H.).

*Tel./Fax: (+86)-378-3886876. E-mail:jyniu@henu.edu.cn (J.N.).

Notes

The authors declare no competing financial interest.

■ **REFERENCES**

(1) (a) Pope, M. T. *Heteropoly and Isopoly Oxometalates*; Springer–Verlag: New York, 1983. (b) Song, Y. F.; Tsunashima, R. *Chem. Soc. Rev.* **2012**, *41*, 7384–7402.

(2) (a) Izarova, N. V.; Pope, M. T.; Kortz, U. *Angew. Chem., Int. Ed.* **2012**, *51*, 9492–9510. (b) Zheng, S. T.; Yang, G. Y. *Chem. Soc. Rev.* **2012**, *41*, 7623–7646.

(3) Mizuno, N.; Kamata, K. *Coord. Chem. Rev.* **2011**, *255*, 2358–2370.

(4) Han, Q. X.; He, C.; Zhao, M.; Qi, B.; Niu, J. Y.; Duan, C. Y. *J. Am. Chem. Soc.* **2013**, *135*, 10186–10189.

(5) Dolbecq, A.; Dumas, E.; Mayer, C. R.; Mialane, P. *Chem. Rev.* **2010**, *110*, 6009–6048.

(6) Dawson, B. *Acta Crystallogr.* **1953**, *6*, 113–126.

(7) (a) Holscher, M.; Englert, U.; Zibrowius, B.; Holderich, W. F. *Angew. Chem., Int. Ed.* **1994**, *33*, 2491–2493. (b) Yin, P. C.; Pradeep, C. P.; Zhang, B. F.; Li, F. Y.; Lydon, C.; Rosnes, M. H.; Li, D.; Bitterlich, E.; Xu, L.; Cronin, L.; Liu, T. B. *Chem.—Eur. J.* **2012**, *18*, 8157–8162.

(8) (a) Yu, L. K.; Yu, Y.; Jiang, B. D.; Zhou, B. B. *Cryst. Eng. Commun.* **2013**, *15*, 5156–5167. (b) Wang, J. P.; Li, S. Z.; Shen, Y.; Niu, J. Y. *Cryst. Growth Des.* **2008**, *8*, 372–374.

(9) Christopher, R. G.; Richard, G. F. *Inorg. Chem.* **2008**, *47*, 3679–3686.

(10) Yang, Y.; Liu, S. X.; Li, C. C.; Li, S. J.; Ren, G. J.; Wei, F.; Tang, Q. *Inorg. Chem. Commun.* **2012**, *17*, 54–57.

(11) Bernardini, G.; Wedd, A. G.; Zhao, C.; Bond, A. M. *Dalton Trans.* **2012**, *41*, 9944–9954.

(12) Herbstein, F. H.; Marsh, R. E. *Acta Crystallogr., Sect. B: Struct. Sci.* **1998**, *54*, 677–686.

(13) (a) Himeno, S.; Saito, A.; Hori, T. *Bull. Chem. Soc. Jpn.* **1990**, *63*, 1602–1606. (b) Kortz, U.; Pope, M. T. *Inorg. Chem.* **1994**, *33*, 5643–5646.

(14) (a) Long, D. L.; Song, Y. F.; Wilson, E. F.; Kögerler, P.; Guo, S. X.; Bond, A. M.; Hargreaves, J. S. J.; Cronin, L. *Angew. Chem., Int. Ed.* **2008**, *47*, 4384–4387. (b) Long, D. L.; Yan, J.; Oliva, A. R.; Busche, C.; Miras, H. N.; Erringtonb, R. J.; Cronin, L. *Chem. Commun.* **2013**, *49*, 9731–9733.

(15) Yan, J.; Long, D. L.; Wilson, E. F.; Cronin, L. *Angew. Chem., Int. Ed.* **2009**, *48*, 4376–4380.

(16) Ozawa, Y.; Sasaki, Y. *Chem. Lett.* **1987**, 923–926.

(17) Jeannin, Y.; Martin-Frere, J. *Inorg. Chem.* **1979**, *18*, 3010–3014.

(18) (a) Long, D. L.; Kögerler, P.; Cronin, L. *Angew. Chem., Int. Ed.* **2004**, *43*, 1817–1820. (b) Long, D. L.; Abbas, H.; Kögerler, P.; Cronin, L. *Angew. Chem., Int. Ed.* **2005**, *44*, 3415–3419.

(19) Partik, M.; Lutz, H. D. *Phys. Chem. Miner.* **1999**, *27*, 41–46.

(20) Street, G.; Minur, Z. *J. Inorg. Nucl. Chem.* **1970**, *32*, 3769–3774.

(21) Kortz, U.; Savelieff, M. G.; Bassil, B. S.; Dickman, M. H. *Angew. Chem., Int. Ed.* **2001**, *40*, 3384–3386.

(22) (a) Hussain, F.; Conrad, F.; Patzke, G. R. *Angew. Chem., Int. Ed.* **2009**, *48*, 9088–9091. (b) Ritchie, C.; Speldrich, M.; Gable, R. W.; Sorace, L.; Kögerler, P.; Boskovic, C. *Inorg. Chem.* **2011**, *50*, 7004–7014.

(23) Sheldrick, G. M. *SHELXTL97, Program for Crystal Structure Solution*; University of Göttingen: Göttingen, Germany, 1997.

(24) *SMART Data collection software (version 5.629)*; Bruker AXS, Inc.: Madison, WI, 2003.

(25) *SAINT, Data reduction software (version 6.45)*; Bruker AXS, Inc.: Madison, WI, 2003.

(26) Data for $C_{18}H_{88}As_2N_{12}Ni_8O_{77}W_{18}$: M_r = 5633.4, triclinic, space group $P\bar{1}$, a = 13.298(5) Å, b = 13.956(6) Å, c = 17.081(7) Å, α = 67.775(4)°, β = 106.093(2)°, γ = 88.789(5)°, V = 2776(2) Å³, Z = 1, $F(000)$ = 2507; of 26985 reflections, 8060 observed, 9771 unique (R_{int} = 0.0362). Final R_1 [with $I > 2\sigma(I)$] = 0.0365, wR_2 (all data) = 0.1137 and S = 1.020.

(27) Li, J.; Huang, Y.; Han, Q. X. *Chin. J. Struct. Chem.* **2013**, *32*, 1897–1903.

(28) Han, Q. X.; Ma, P. T.; Zhao, J. W.; Wang, J. P.; Niu, J. Y. *Inorg. Chem. Commun.* **2011**, *14*, 767–770.

(29) Zhao, J. W.; Han, Q. X.; Shi, D. Y.; Chen, L. J.; Ma, P. T.; Wang, J. P.; Niu, J. Y. *J. Solid State Chem.* **2011**, *184*, 2756–2761.

(30) (a) Wang, B.; Bi, L. H.; Wu, L. X. *J. Mater. Chem.* **2011**, *21*, 69–71. (b) Richardt, P. J. S.; Gable, R. W.; Bond, A. M.; Wedd, A. G. *Inorg. Chem.* **2001**, *40*, 703–709. (c) Way, D. M.; Cooper, J. B.; Sadek, M.; Vu, T.; Mahon, P. J.; Bond, A. M.; Brownlee, R. T. C.; Wedd, A. G. *Inorg. Chem.* **1997**, *36*, 4227–4233.

(31) (a) Rusanov, E. B.; Ponomarova, V. V.; Komarchuk, V. V.; Stoeckli-Evans, H.; Fernandez-Ibanez, E.; Stoeckli, F.; Sieler, J.; Domasevitch, K. V. *Angew. Chem., Int. Ed.* **2003**, *42*, 2499–2501. (b) Mantero, D. G.; Neels, A.; Stoeckli-Evans, H. *Inorg. Chem.* **2006**, *45*, 3287–3294. (c) Degtyarenko, A. S.; Solntsev, P. V.; Krautscheid, H.; Rusanov, E. B.; Chernegac, A. N.; Domasevitch, K. V. *New J. Chem.* **2008**, *32*, 1910–1918.

(32) (a) Gjikaj, M.; Wu, P.; Brockner, W. *Z. Anorg. Allg. Chem.* **2012**, *638*, 2144–2149. (b) Szklarz, P.; Chański, M.; Ślepokura, K.; Lis, T. *Chem. Mater.* **2011**, *23*, 1082–1084. (c) Haag, J. M.; LeBret, G. C.; Cleary, D. A.; Twamley, B. *J. Solid State Chem.* **2005**, *178*, 1308–1311.

(33) (a) Chen, C.; Zhao, W.; Lei, P.; Zhao, J.; Serpone, N. *Chem.—Eur. J.* **2004**, *10*, 1956–1965. (b) Zou, C.; Zhang, Z. J.; Xu, X.; Gong, Q. H.; Li, J.; Wu, C. D. *J. Am. Chem. Soc.* **2012**, *134*, 87–90.

(34) Pang, H. J.; Ma, H. Y.; Peng, J.; Zhang, C. J.; Zhang, P. P.; Su, Z. M. *Cryst. Eng. Commun.* **2011**, *13*, 7079–7085.

(35) Yang, H. X.; Liu, T. F.; Cao, M. N.; Li, H. F.; Gao, S. Y.; Cao, R. *Chem. Commun.* **2010**, *46*, 2429–2431.

(36) (a) Ismail, A. H.; Dickman, M. H.; Kortz, U. *Inorg. Chem.* **2009**, *48*, 1559–1560. (b) Hao, J.; Xia, Y.; Wang, L. S.; Ruhlmann, L.; Zhu, Y. L.; Li, Q.; Yin, P.; Wei, Y. G.; Guo, H. Y. *Angew. Chem., Int. Ed.* **2008**, *47*, 2626–2630.

(37) Sattari, D.; Hill, C. L. *J. Am. Chem. Soc.* **1993**, *115*, 4649–4651.

(38) $K_6As_2W_{18}O_{62}$ was prepared according to the literature: Acerete, R.; Hammer, C. F.; Baker, L. C. W. *Inorg. Chem.* **1984**, *23*, 1478–1482.